

*Phys. Chem. Res.*, Vol. 5, No. 3, 483-496, September 2017  
DOI: 10.22036/pcr.2017.63757.1315

## Molecular Dynamics Simulation and Free Energy Studies on the Interaction of Salicylic Acid with Human Serum Albumin (HSA)

L. Karami<sup>a</sup>, E. Tazikeh-Lemeski<sup>b,\*</sup> and A.A. Saboury<sup>c</sup>

<sup>a</sup>Department of Cell and Molecular Biology, Faculty of Biological Sciences, Kharazmi University, Tehran, Iran

<sup>b</sup>Department of Chemistry, Gorgan Branch, Islamic Azad University, Gorgan, Iran

<sup>c</sup>Institute of Biochemistry and Biophysics, University of Tehran, Tehran, Iran

(Received 20 October 2016, Accepted 15 January 2017)

The most important protein in the blood plasma is Human serum albumin (HSA). Molecular dynamics simulations of subdomain IIA of HSA and its complex with salicylic acid (SAL) were performed to investigate structural changes induced by the ligand binding. To estimate the binding affinity of SAL molecule to subdomains IB and IIA in HSA protein, binding free energies were calculated using the Molecular Mechanics-Generalized Born Surface Area (MM-GBSA). It was found that the presence of SAL molecule leads to the stability of HSA. Also, ligand binding decreases the  $\alpha$ -helix content of HSA. Binding free energy calculations demonstrate that the binding affinity of the SAL molecule to subdomain IIA of HSA is more than that of subdomain IB of HSA, and the contributions of van der Waals interactions are more than that of electrostatics interactions. The per-residue decomposition of binding free energy suggested that the favorable residues with the most contribution in the binding free energy are hydrophobic, contributing to van der Waals interactions. Our important finding is that the subdomain IIA of HSA is the main HSA-SAL binding site. The results obtained are in good agreement with the corresponding experimental data.

**Keywords:** Molecular dynamics simulations, Binding free energy, Human serum albumin, Salicylic acid, Molecular mechanics-generalized born surface area

### INTRODUCTION

Human Serum Albumin (HSA), which is synthesized in the liver, is the most common protein in plasma [1,2]. The hydrophobic pockets in HSA protein play a prominent role in the transportation of various kinds of ligands including hemin and fatty acids [3,4], bilirubin (toxic metabolite derived from heme) [5,6] and other molecules such as drugs.

The study of the interaction between drugs and HSA protein is of a great importance in drug delivery and the mechanism of therapeutic effect. Therefore, these conformational changes should be taken into consideration

when analyzing drug interactions at albumin binding level [7-10].

The three-dimensional structure of HSA has been detected by X-ray crystallography method [11]. This heart-shaped molecule has an average thickness of 30 Å and a volume of 88249 Å<sup>3</sup> (the secondary structure is shown in Fig. 1a). The structure of this protein is composed of three homologous domains (I,II,III) that each domain is comprised of two subdomains (A,B) which are predominantly helical and extensively cross-linked by several disulfide bridges [12,13]. The presence of the large number of charged amino acids (31%) in HSA structure reflects facility of interaction of this protein with anionic and cationic ligands (like drugs). The ligand binding site in HSA is located in the hydrophobic regions of subdomains

\*Corresponding author. E-mail: [elham\\_tazike@yahoo.com](mailto:elham_tazike@yahoo.com)

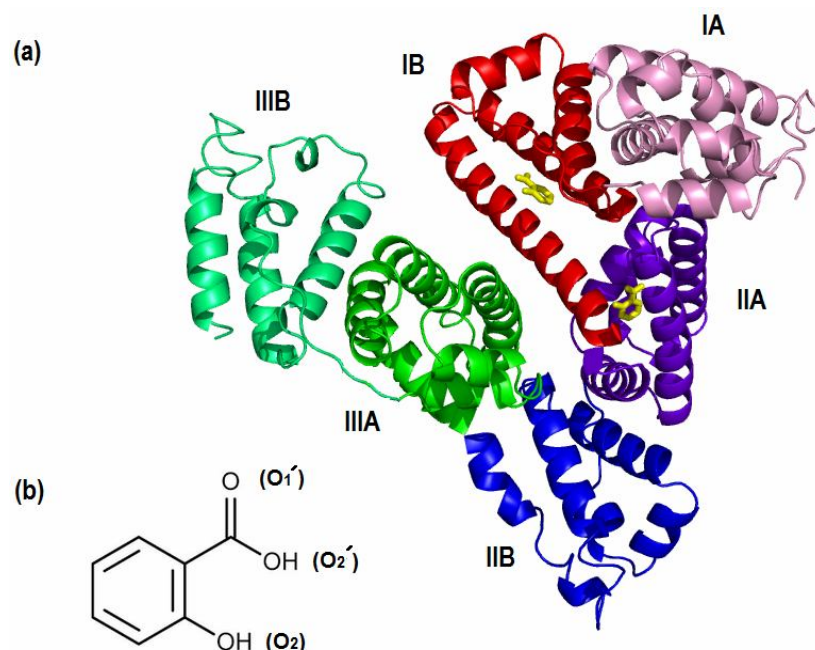


**Fig. 1.** (a) Secondary structure of Human Serum Albumin (HSA, PDB code: 2I30). Domains, subdomains and SAL molecules are shown in different colors; IA: pink, IB: red, IIA: purple, IIB: blue, IIIA: green, IIIB: cyan, SAL: yellow, (b) Chemical structure of Salicylic acid (SAL).

IIA (site I) and IIIA (site II) [14-16].

The hydrophobic interactions with neutral heterocyclic compounds and the van der Waals interactions with aromatic carboxylic acids are involved in site I and site II, respectively. Hence, these interactions provide HSA with the potential ability to bind to many organic and inorganic molecules.

Non-steroidal anti-inflammatory drugs (NSAID) are among the most important drugs transported using HSA protein [17]. Pain-reduction, fever-reduction, and even anti-inflammation are of the effects of NSAIDs usage [18,19].

The most common NSAIDs are aspirin, ibuprofen and naproxen. Aspirin, or acetylsalicylic acid (ASA) is a salicylate drug which is generally used as an analgesic for minor aches and pains to reduce fever and also as an anti-inflammatory drug. Besides, aspirin has turned increasingly into popular anti-platelet used to prevent blood clot formation, in long-term low doses. Unlike other NSAIDs, aspirin irreversibly inhibits cyclooxygenase COX enzyme [20], resulting in the longer effect time.

Due to high ligand binding ability, many investigators have studied the genetics and metabolism of HSA using a wide range of experimental techniques. In 2007, Tajmir-Riahi [21] mentioned to studies in which structural analysis of HSA complexes, with different ligand, especially drugs have reported. In this review article, the results of several studies on the interaction of HSA with different drugs, such as quercetin (antioxidant), kaempferol (antioxidant), AZT (30-azido-30-deoxythymidine) (anti-AIDS), aspirin (anti-inflammatory), taxol (anticancer), cisplatin (anticancer) and chlorophyllin (antitumor) [22-27] are discussed in aqueous solution. In these studies, drug binding mode, the binding constant and the stability and protein secondary structural changes have been determined using CD (Circular dichroism), capillary electrophoresis, FTIR (Fourier transform infrared) and UV-Vis spectroscopic methods. These studies indicate that the hydrophobic interactions play the main role in the interaction between HSA and most of the drugs [28]. One of the main changes in the protein structure is partial unfolding in these HSA-drug complexes caused by reduction of  $\alpha$ -helix and enhancement of  $\beta$ -

structures [21].

Recently, the molecular dynamics (MD) computations have been applied in the molecular level of protein-ligand interactions. In 2005, Artali *et al.* [29] performed a molecular dynamics study on the HSA to elucidate the geometric and dynamic properties of the HSA binding sites. Li *et al.* investigated the binding of HSA to angiotensin II receptor blockers (ARBs) using docking and molecular dynamics simulations. Their results demonstrate that the main HAS-ARB binding site is subdomain IIIA of HSA [30]. In 2010, Sudhamalla *et al.* [31] used both of experimental (fluorescence, circular dichroism) and computational methods to study the interaction of  $\beta$ -sitosterol with HSA. In 2013, Castellanos and Colina considered molecular dynamics simulations of HSA to provide information on the relevance of disulfide bonds in the dynamics and structural conformation of HSA. They found that conformational changes are observed in the absence of disulfide bonds that could impact the functionality and stability of the protein [32]. Recently, Mozafari *et al.* [33] investigated the thermodynamic parameters and the structural changes of HSA protein induced by indomethacin drug combination by means of isothermal titration calorimetry technique and MD simulation computations, simultaneously.

Molecular dynamics simulation methods can substitute for some of the experimental techniques, since it provides valuable information about the atomic details in different time scales.

It's crucial to investigate the binding effect of aspirin on HSA, due to its important role in biological systems. In this study, salicylic acid molecule (SAL) was considered as a representative of aspirin molecule. Calculations were carried out in two phases: first, to investigate conformational and structural changes induced by the ligand binding, molecular dynamics simulations of free HSA and HSA-SAL complex were performed, and second, to estimate the binding free energy from molecular simulations, molecular mechanics generalized Born surface area (MM-GBSA) method was used. Our study is, to the best of our knowledge, the first one to provide a more detailed picture of the structural effects of the aspirin on HSA using the MD simulations. In the following sections, first, the simulation details are described; then, the results of

the simulations are discussed. Finally, the conclusions related to the simulated systems are expressed.

## COMPUTATIONAL DETAILS

### Simulation System

The starting structure of HSA protein was obtained from the Protein Data Bank (PDB code 2I30) [34], which is in complex with the myristate and salicylic acid (SAL). All myristate ligands were eliminated. There are two SAL molecules in this PDB file; one at IB subdomain and another at IIA subdomain. We considered and prepared three model systems: (i) subdomain IB-SAL complex (ii) subdomain IIA (iii) subdomain IIA-SAL complex. Based on experimental data [12,13], aspirin binds to subdomains IIA and IIIA in HSA structure. Subdomain IIA is one of the main drug binding sites on HSA protein, thus, we only considered the effect of SAL molecule on the subdomain IIA for MD simulation. To investigate structural changes induced by the ligand binding, molecular dynamics simulations of subdomain IIA and subdomains IIA-HSA complex models were performed and then compared. In the second part of study, to estimate the binding affinity of SAL molecule to subdomains IB and IIA in HSA protein, binding free energies were calculated using MM-GBSA method.

### Simulation Protocol

All simulations were carried out using the AMBER10 suite of program [35] with the ff03 force field [36] for the protein (HSA) and the gaff force field [37] for the ligand (SAL). Hydrogen atoms were added to the subdomain IIA in free and bound states using the AMBER all-atom data base. The structure was placed into a rectangular periodic box of TIP3P [38] in which, the distance between the closest atom of the solute and the edges of the box was at least 12 Å in all directions. The Cl<sup>-</sup> counter ions were added to maintain the electro neutrality of the systems using the leap program from the AMBER10 package. AM1-BCC charges [39] were assigned to the ligand using the antechamber module from the AMBER10 package. Periodic boundary conditions (PBC) in all directions and the particle mesh Ewald (PME) method [40] for long-range electrostatic interactions were applied. The cutoff distance for non-bonded interactions was set to 10 Å. Initial velocities were

designated from Maxwell-Boltzmann distribution. All bonds containing hydrogen atoms were constrained using the SHAKE algorithm [41]. The time step for all MD simulations was set to 2 fs. In all of the simulations, the temperature and pressure were controlled by the Langevin temperature coupling scheme and the isotropic position scaling protocol [42], respectively.

The following protocol was carried out for all MD simulations: First, 2000-step steepest descent minimization was performed. Afterward, system was heated from 0 to 298 K through a canonical ensemble (NVT)-MD simulation for 200 ps. To adjust the solvent density, a short simulation (100 ps) was applied in the NPT ensemble. In these three steps, minimization and MD simulation were performed with position restraints of  $1000 \text{ kJ mol}^{-1} \text{ nm}^{-2}$  on the all solute atoms. Then, 500 ps NPT equilibration without position restraint was carried out. Finally, a production run was performed for 10 ns under conditions of constant pressure and temperature. In equilibration and production run steps, temperature and pressure are assigned 298 K and 1 bar, respectively. The atomic coordinates were saved every 0.5 ps for the analysis, resulting in a total of 2000 snapshots. Molecular graphics were made with the Pymol program [43].

### Free Energy Calculations

There are various methods to calculate binding free energy, such as thermodynamic integration (TI) [44], free energy perturbation (FEP) [45] and linear interaction energy (LIE) [46]. The alternative approach, molecular mechanics generalized Born surface area (MM-GBSA) method [47, 48] is more computationally efficient. This post-processing method uses minimized snapshots collected from the MD trajectories. This method combines molecular mechanical (MM) energies with a continuum solvent generalized Born (GB) model for polar solvation and with a solvent-accessible surface area (SASA) [49] for non-polar solvation term. Entropy contribution was estimated using normal-mode analysis [50,51] or a quasi-harmonic approximation [52]. This method has been widely and successfully employed [47,53,54] to calculate binding affinity for protein-ligand and protein-peptide interactions.

The binding free energies ( $\Delta G_{\text{bind}}$ ) between a protein and a ligand were calculated using the MM-GBSA method that

have been shown in our recent studies [33,55].

The main equations are shown as below:

$$\Delta G_{\text{bind}} = G_{\text{complex}} - (G_{\text{protein}} + G_{\text{ligand}}) \quad (1)$$

Each of these free energies can be broken down into the following terms:

$$G_i = E_{\text{MM}} + G_{\text{sol}} - TS \quad (2)$$

$E_{\text{MM}}$ : the gas-phase interaction energy between the protein and the ligand is calculated by summing the amounts of the internal ( $E_{\text{int}}$ ), electrostatic ( $E_{\text{ele}}$ ) and van der Waals, ( $E_{\text{vdw}}$ ) interaction energies.

$G_{\text{sol}}$ : the solvation free energy is calculated by adding polar ( $G_{\text{pol}}$ ) and non-polar ( $G_{\text{nonpol}}$ ) energies.

$T$ : the absolute temperature

$S$ : the solute entropy is a combination of three components; translational ( $S_{\text{trans}}$ ), rotational ( $S_{\text{rot}}$ ), and vibrational ( $S_{\text{vib}}$ ) entropies.

The sander module, from the AMBER10 package, was applied to calculate molecular mechanical gas phase energies. In the MM-GBSA method, internal and external dielectric constants of 1 and 80, were employed, respectively. The Parse set of radii was used for all atoms. The solvent probe radius was set at 1.4 Å. The Onufriev's GB model [56] was applied for GB calculations. To calculate the solvent accessible surface area (SASA) in the nonpolar solvation energy,  $G_{\text{nonpol}}$ , the molsurf program was used [57]. The solute entropy,  $S$ , was estimated by normal mode analysis performed with the AMBER NMODE module.

Owing to the high computational demand, normal mode calculations were carried out only for every fifth one of the last 200 snapshots. The maximum number of minimization cycles was set to 10000. The convergence criterion for the energy gradient to stop minimization was 0.0001. To provide useful insights into the important interactions in free energy calculations, we decomposed the contributions to binding free energies on a per-residue basis [58].

## RESULTS AND DISCUSSION

To investigate structural changes induced by the ligand

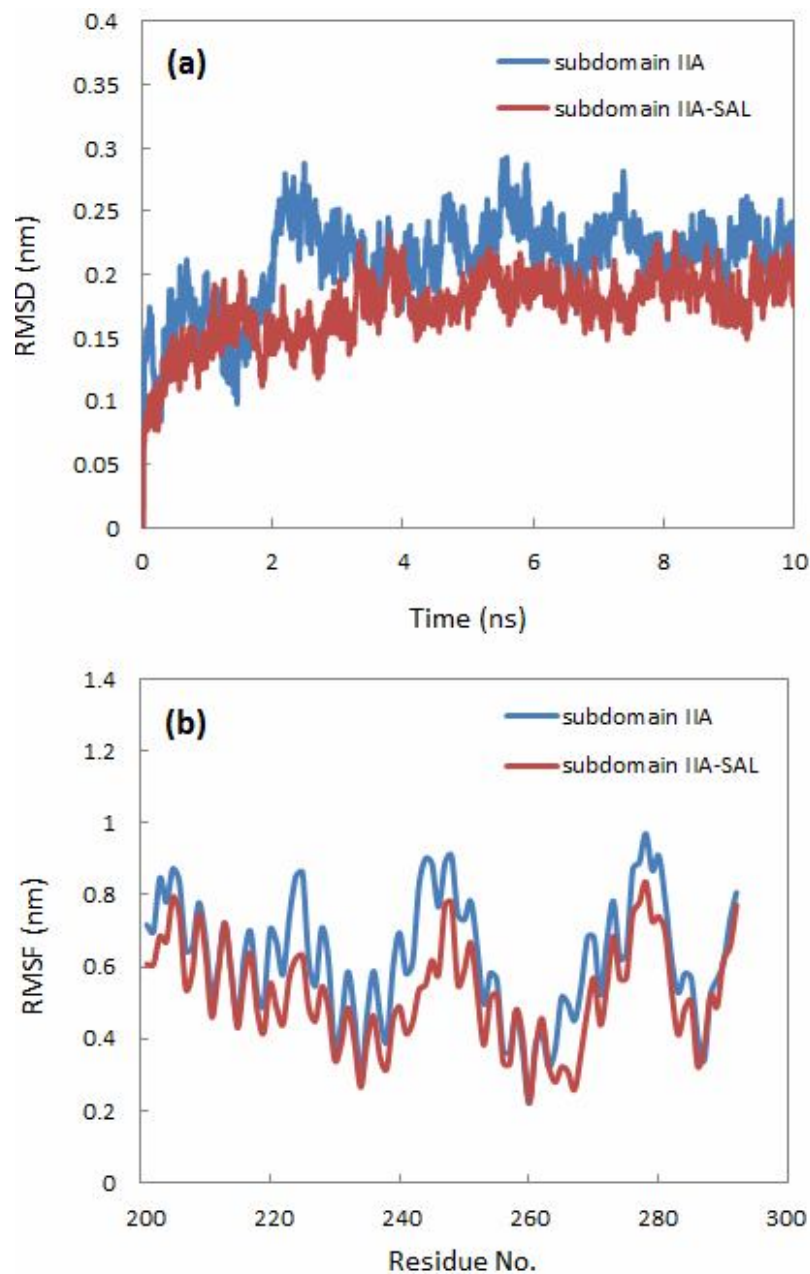


**Fig. 2.** (a) Root mean square deviation (RMSD) measured from the corresponding starting structure in HSA structure, (b) Root mean square fluctuation (RMSF) around the average MD structure.

(SAL) binding, molecular dynamics simulations of free HSA (subdomain IIA) and subdomain IIA-SAL complex were performed and then compared. The root mean square deviations (RMSD), root mean square fluctuations (RMSF) and secondary structure were investigated as a measure of

the structural properties. Using these properties, the stability of the HSA protein can be qualitatively compared during the simulation time. The time evolution of RMSD from the initial structure was calculated for two production run simulations (subdomain IIA and subdomain IIA-SAL

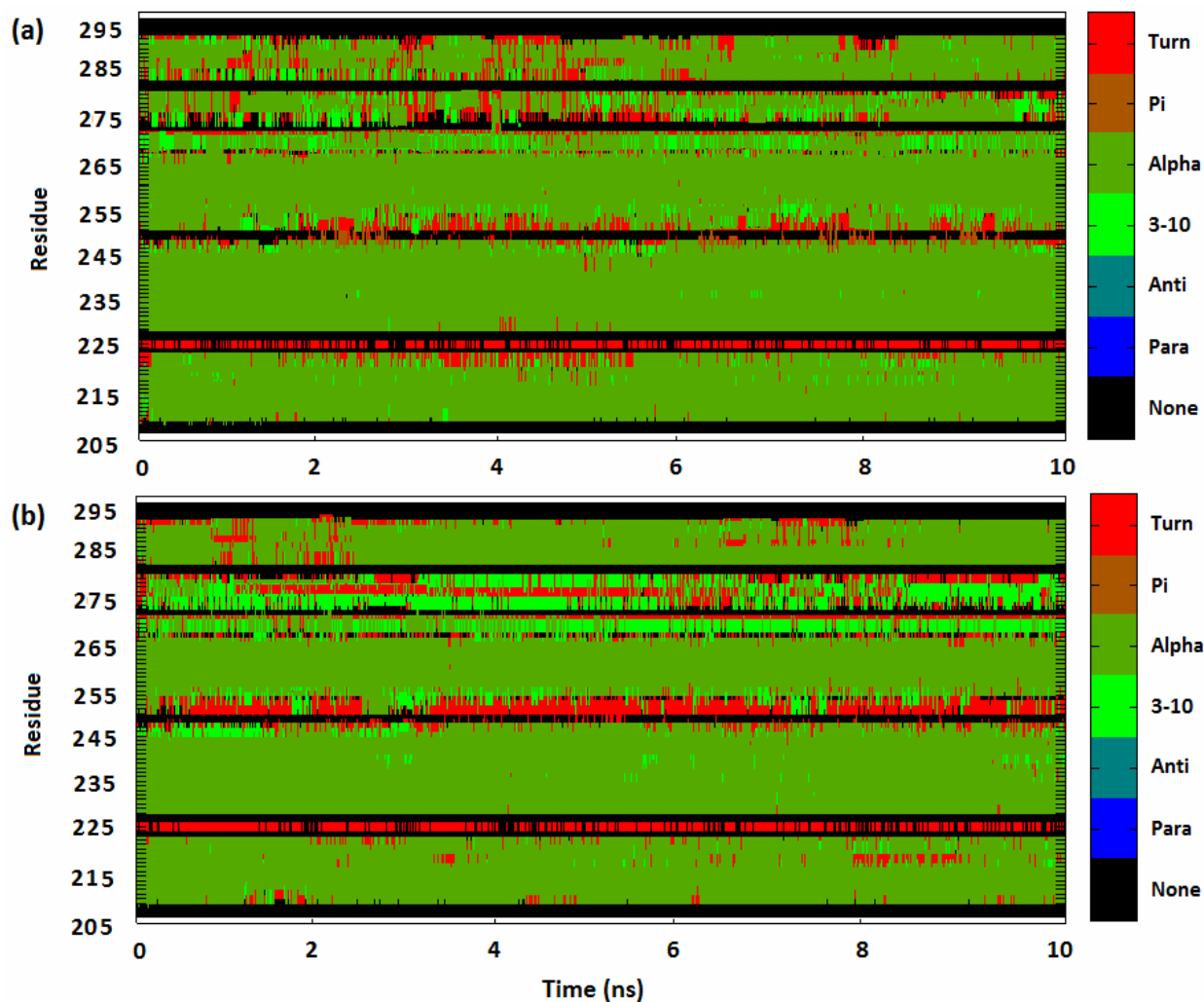


**Fig. 2.** (a) Root mean square deviation (RMSD) measured from the corresponding starting structure in HSA structure, (b) Root mean square fluctuation (RMSF) around the average MD structure.

complex). RMSDs of the protein C $\alpha$  atoms are plotted in Fig. 2a showing RMSD for subdomain IIA and subdomain IIA in complex with SAL. Both of the free protein and protein in complex become stable after 2.5 ns, suggesting an equilibrated system. The RMSD value of the HSA protein fluctuated around 0.23 nm in free protein and 0.18 nm in the protein-ligand complex. As shown in Fig. 2a, RMSD values for protein C $\alpha$  atoms are reduced upon binding. Ligand binding and consequent restriction of the molecular motions cause the decrease of RMSD value of protein in complex with respect to free protein. Since distance deviations from

the starting structure may not necessarily reflect the mobility of structural elements, another parameter, RMSF, is used to obtain information on flexibility. To identify flexible regions in the molecule, RMSFs of the protein C $\alpha$  atoms are illustrated in Fig. 2b. As shown in this figure, RMSF for free protein and protein in complex with ligand has similar trend, and in both states, the residues 248-256 and 263-282 have highest values of the RMSF. Owing to the restriction of molecular motions resulting from ligand binding, the protein in the complex with ligand (SAL) shows the lower RMSF values relative to the free protein.

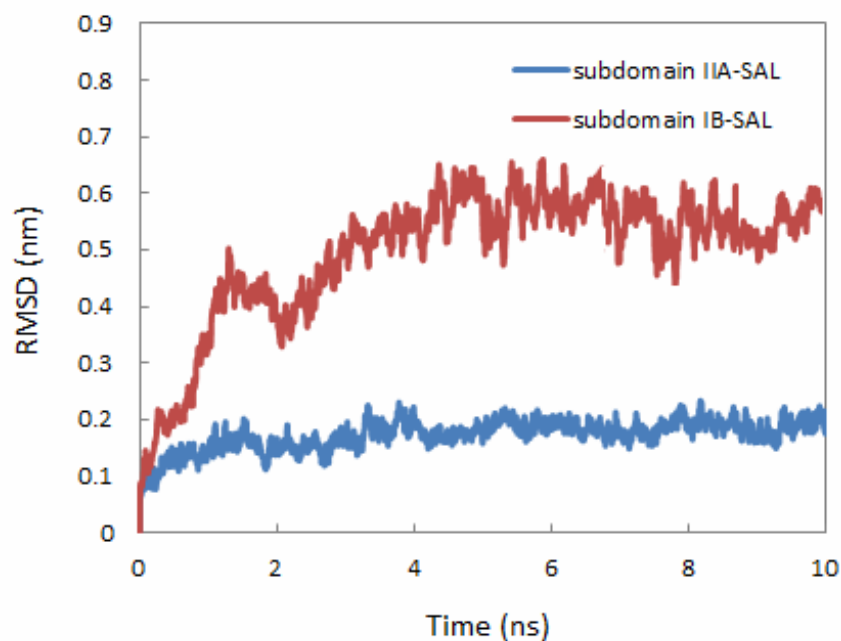


**Fig. 4.** Root mean square deviation (RMSD) measured from the corresponding starting structure for subdomain IB-SAL and subdomain IIA-SAL complexes.

The analysis of secondary structure was done with the DSSP program [59]. The secondary structures of free protein (subdomain IIA) and protein in complex with ligand (subdomain IIA-SAL complex) as a function of time are depicted in Fig. 3a and Fig. 3b, respectively. To distinguish between the secondary structure types, different colors were used. The overall secondary structure pattern of free (Fig. 3a) and bound HSA (Fig. 3b) is maintained during the 10 ns MD simulation, although there was a slight change at some points as a function of time. These changes are often seen in the residues 265-291. With a glance to Fig. 3, it can be understood that the major secondary structure of PRH in both trajectories is as  $\alpha$ -helix, and residues 208-219, 227-244 and 255-264 keep their  $\alpha$ -helicity throughout the 10 ns MD simulation, in free and bound state. As shown in Fig. 3, ligand binding decreases  $\alpha$ -helix content of HSA, especially in residues 247-255 and 267-280 which is in agreement with experimentally observed results [21,60].

The subdomain IB-SAL and subdomain IIA-SAL complexes are investigated structurally and thermodynamically. To explore the dynamic stability of two HSA-SAL complexes, the time evolution of RMSD from the initial structures was calculated for the protein C $\alpha$  atoms

and plotted in Fig. 4. The RMSD profiles for subdomain IIA-SAL complex were continually less than 0.18 nm during the all simulation time suggesting the high stability of this system. As can be seen from Fig. 4, the RMSD values of the protein C $\alpha$  atoms for the subdomain IB-SAL complex are higher than that of subdomain IIA-SAL complex. The RMSD plots indicate that the subdomain IIA-SAL achieve equilibrium much faster than that of the subdomain IB-SAL complex. The differences observed in the RMSD profiles of the HSA-SAL complexes imply the higher stability of the subdomain IIA-SAL complex relative to the subdomain IB-SAL complex. In addition to RMSD, RMSF for the protein C $\alpha$  atoms were calculated (data not shown). The average RMSF per residue for the subdomain IB-SAL and subdomain IIA-SAL complexes are 0.52, 0.44, respectively. The relatively larger RMSF per residue of the subdomain IB-SAL complex can be easily explained by the relatively weaker binding of SAL molecule to subdomain IB of HSA protein. To estimate the binding affinity of SAL molecule to subdomains IB and IIA in HSA protein, binding free energies were calculated using MM-GBSA method to complement the structural analysis. To obtain the mean values of binding free energies with reasonable precision

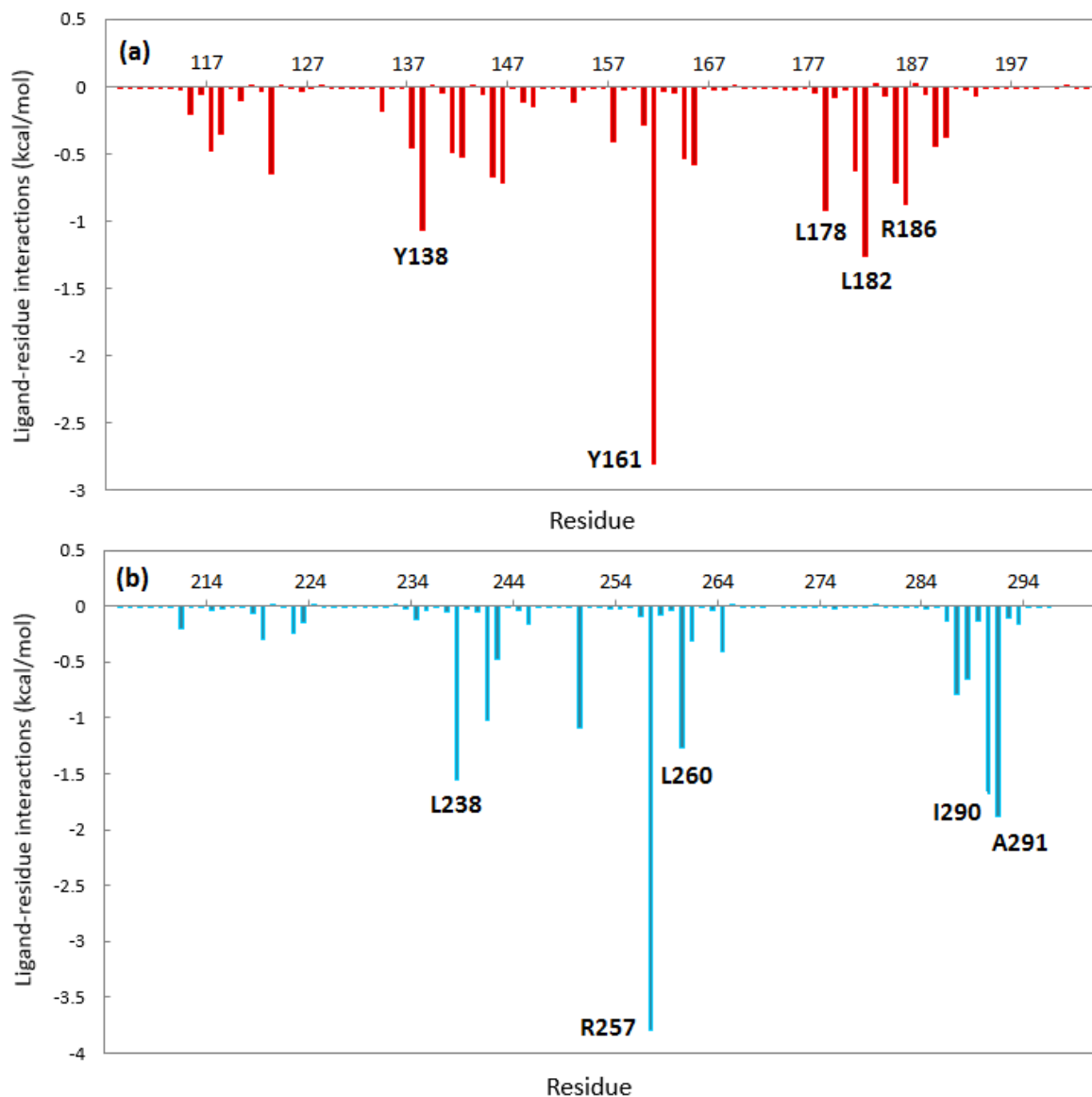


**Fig. 5.** Ligand-residue interaction spectrum of (a) the subdomain IB-SAL complex and (b) the subdomain IIA-SAL complex according to the MM-GBSA method. The *x*-axis indicates the residue number of HSA and the *y*-axis denotes the interaction energy between the SAL molecule and specific residues.

[61,62], a total of 200 snapshots were collected from the last 2.5 ns of MD simulations of the HSA-SAL complexes. Normal-mode analysis was used to calculate the entropy contributions based on a harmonic approximation after energy minimization of the snapshots. Table 1 represents the calculated results. The calculated binding free energies for subdomain IB-SAL and subdomain IIA-SAL complexes

are 3.02 and -1.66 kcal mol<sup>-1</sup>, respectively. The energy compon. The calculated binding free energies for subdomain IB-SAL and subdomain IIA-SAL complexes are 3.02 and -1.66 kcal mol<sup>-1</sup>, respectively. The energy compSAL complexes, the time evolution of RMSD from the initial structures was calculated for the protein *C* $\alpha$  atoms and plotted in Fig. 4. The RMSD profiles for subdomain

**Table 1.** Calculated Binding Free Energies and their Components for HSA-SAL Complexes

Energy (kcal mol <sup>-1</sup> )	Subdomain IB-SAL		Subdomain IIA-SAL	
	Mean	$\sigma^a$	Mean	$\sigma^a$
$\Delta E_{\text{ele}}$	-4.93	0.29	-2.40	0.29
$\Delta E_{\text{vdw}}$	-17.17	0.18	-18.59	0.21
$\Delta E_{\text{MM}}$	-22.09	0.35	-20.99	0.34
$\Delta G_{\text{pol (GB)}}$	13.12	0.24	13.41	0.26
$\Delta G_{\text{nonpol (SA)}}$	-2.63	0.02	-2.72	0.02
$\Delta G_{\text{sol (GBSA)}}$	10.49	0.23	10.68	0.26
$\Delta G_{\text{MM-GBSA}}$	-11.60	0.18	-10.31	0.18
$T\Delta S_{\text{trans}}$	-12.11	0.00	-12.11	0.00
$T\Delta S_{\text{rot}}$	-8.74	0.00	-8.71	0.02
$T\Delta S_{\text{vib}}$	6.23	0.72	12.17	5.49
$-T\Delta S_{\text{total}}$	14.62	0.74	8.65	5.51
$\Delta G_{\text{binding}}$	3.02		-1.66	

<sup>a</sup>Standard error of the mean.

IIA-SAL complex were continually less than 0.18 nm during the all simulation time, suggesting the high stability of this system. As can be seen from Fig. 4, the RMSD values of the protein C $\alpha$  atoms for the subdomain IB-SAL complex are higher than that of subdomain IIA-SAL complex. The RMSD plots indicate that the subdomain IIA-SAL achieve equilibrium much faster than that of the subdomain IB-SAL complex. The differences observed in the RMSD profiles of the HSA-SAL complexes imply the higher stability of the subdomain IIA-SAL complex relative to the subdomain IB-SAL complex. In addition to RMSD, RMSF for the protein C $\alpha$  atoms were calculated (data not shown). The average RMSF per residue for the subdomain IB-SAL and subdomain IIA-SAL complexes are 0.52, 0.44, respectively. The relatively larger RMSF per residue of the subdomain IB-SAL complex can be easily explained by the relatively weaker binding of SAL mole subdomain IB-SAL and subdomain IIA-SAL complexes are investigated structurally and thermodynamically. To explore the

dynamic stability of two HSA-Due to the importance of the hydrogen bonds interactions in the formation of the protein-ligand complexes, the hydrogen bonds were studied in the HSA-SAL complexes. Only intermolecular hydrogen bonds are investigated. For the hydrogen bond analysis, we defined a geometric criterion for a hydrogen bond D-H $\cdots$ A, where A is acceptor, D is the donor atom, and H is the hydrogen atom: an acceptor-donor pair is considered to form a hydrogen bond if the donor-acceptor distance ( $d_{DA}$ )  $\leq 3.5$  Å and the donor-hydrogen-acceptor angle ( $\alpha_{DHA}$ )  $\geq 135^\circ$ . In SAL molecule, OH groups are as hydrogen bond donor and acceptor, whereas the oxygen atom (O $_1$ ) is only as a hydrogen bond acceptor (see Fig. 1b). The hydrogen bond analysis shows that the number and occupancy of the hydrogen bonds in subdomain IIA-SAL complex is greater than those of subdomain IB-SAL complex, indicating the higher stability of subdomain IIA-SAL complex relative to subdomain IB-SAL complex (see Fig. 6a and Table 2). Average number of hydrogen bonds is 37 and 44 for IB-

**Table 2.** HSA-SAL Hydrogen Bonds Observed in MD Simulation<sup>a</sup>

Donor	Donor_H	Acceptor	Occupancy (%) <sup>b</sup>	Average distance	Average angle
Subdomain IB-SAL					
TYR_138@OH	TYR_138@HH	SAL@O2	73	2.88	158.16
SAL@O2'	SAL@HO2'	GLU_141@OE2	70	2.83	156.58
TYR_161@OH	TYR_161@HH	SAL@O1'	66	2.85	153.67
TYR_161@OH	TYR_161@HH	SAL@O2'	61	2.76	149.46
TYR_161@OH	TYR_161@HH	SAL@O2	58	2.69	147.15
SAL@O2	SAL@HO2	LYS_181@O	43	2.77	150.02
LYS_137@NZ	LYS_137@HZ1	SAL_98@O1'	55	2.72	149.17
TYR_138@OH	TYR_138@HH	SAL@O1'	52	2.74	155.24
LYS_137@NZ	LYS_137@HZ2	SAL@O1'	46	2.76	146.14
LYS_137@NZ	LYS_137@HZ3	SAL@O1'	44	2.79	147.33
Subdomain IIA-SAL					
SAL@O2'	SAL@HO2'	ARG_257@O	93	2.77	157.82
SAL@O2'	SAL@HO2'	SER_287@O	90	2.69	160.22
ARG_257@NH2	ARG_257@HH21	SAL@O1'	88	2.84	148.04
ARG_257@NE	ARG_257@HE	SAL@O1'	88	2.86	153.51
SAL@O2'	SAL@HO2'	HIE_288@ND1	85	2.86	155.86
SAL@O2	SAL@HO2	SER_287@O	84	2.75	142.72
ARG_257@NE	ARG_257@HE	SAL@O2'	81	2.94	150.76
SAL@O2'	SAL@HO2'	SER_287@O	76	2.86	157.08
ARG_257@NE	ARG_257@HE	SAL@O2	72	2.93	161.20
SER_287@OG	SER_287@HG	SAL@O1'	65	2.87	151.62
ARG_257@NH2	ARG_257@HH21	SAL@O2	61	2.74	135.53
ARG_257@NH1	ARG_257@HH11	SAL@O2	58	2.83	144.79
ARG_257@NH2	ARG_257@HH21	SAL@O2'	56	2.89	153.74
SAL@O2'	SAL@HO2'	ALA_261@N	43	2.94	137.92

<sup>a</sup>Only contacts populated >40% in the last 5 ns of the trajectory are listed. <sup>b</sup>Data was sorted by %occupancy.

SAL and IIA-SAL complexes, respectively. The important amino acids involved in hydrogen bond interactions are Tyr138, Glu141, Tyr161 and Lys181 in subdomain IB-SAL complex and Arg257, Ser287 and His288 in subdomain IIA-SAL complex. Some of these important hydrogen bond interactions for HSA-SAL complexes are depicted in Fig. 6b and 6c.

## CONCLUSIONS

Molecular dynamics simulations and free energy calculations for the SAL molecule binding to the IB and IIA subdomains of HSA protein have been performed to investigate conformational and structural changes induced by the ligand binding on the HSA structure and to compare the binding affinity of the SAL molecule to the IB and IIA subdomains of HSA protein.

In the first part of the study, two MD simulations of 10 ns were performed for the free HSA (subdomain IIA) and subdomain IIA-SAL complex. Structural properties such as the RMSD, RMSF and the secondary structure of protein were evaluated from these trajectories. SAL binding to the IIA subdomain of HSA protein resulted in the stability of the HSA. Analysis of secondary structure indicates a decrease in the  $\alpha$ -helix content of HSA upon ligand binding. This finding is in agreement with experimental results [21, 60]. In the second part of the study, binding free energies of the SAL molecule to the IB and IIA subdomains of HSA protein were investigated using MM-GBSA method. The analysis of energetic contributions to the binding free energy has revealed that in both complexes, the van der Waals term is the major favorable contributor to ligand binding, while the solvation and entropy terms disfavor binding. The calculated binding free energies indicated that affinity of the SAL molecule to IIA subdomain is more than that of IB subdomain. In 2011, Rezaei *et al.* [60] experimentally showed that the binding affinity of Aspirin to IIA subdomain is greater than that of IIIA subdomain of HSA. They showed that IIA subdomain is main binding site for Aspirin. On the basis of our computational study, the binding affinity of SAL to IIA subdomain is greater than that of IB subdomain of HSA. We showed that IIA subdomain is main binding site for SAL. The results obtained are in good agreement with the corresponding

experimental data (IIA subdomain is the main binding site for SAL and Aspirin).

The per-residue decomposition of binding free energy was performed and the favorable residues with the most contribution in the binding free energy were found. These residues are hydrophobic, contributing to van der Waals interactions with the SAL molecule. Moreover, structural analysis (RMSD and RMSF) shows that subdomain IIA-SAL complex is more stable than subdomain IB-SAL complex. These data are in good consistency with the results obtained from the binding free energy and hydrogen bonds analysis.

## ACKNOWLEDGMENTS

This study has been supported by the Gorgan Branch, Islamic Azad University.

## REFERENCES

- [1] Peters, T., Serum albumin. *Adv. Protein. Chem.* **1985**, 37, 161-245. DOI: 10.1016/S0065-3233(08)60065-0.
- [2] Peters, J. T., All about albumin. Biochemistry, genetics and medical applications. Academic Press: 1996
- [3] Zunszain, P. A.; Ghuman, J.; Komatsu, T.; Tsuchida, E.; Curry, S., Crystal structural analysis of human serum albumin complexed with hemin and fatty acid. *BMC Struct. Biol.* **2003**, 3, 6-14. DOI: 10.1186/1472-6807-3-6.
- [4] Curry, S.; Mandeikow, H.; Brick, P.; Franks, N., Crystal structure of human serum albumin complexed fatty acids reveals an asymmetric distribution of binding sites. *Nat. Struct. Biol.* **1998**, 5, 827-835. DOI: 10.1038/1869.
- [5] Petersen, C. E.; Ha, C. E.; Harohalli, K.; Feix, J. B.; Bhagavan, N. V., A dynamic model for bilirubin binding to HSA. *J. Biol. Chem.* **2000**, 275, 20985-20995. DOI: 10.1074/jbc.M001038200.
- [6] Moosavi-Movahedi, Z.; Bahrami, H.; Zahedi, M.; Mahnam, K.; Chamani, J.; Safarian, Sh.; Saboury, A. A.; Moosavi-Movahedi, A. A., Theoretical elucidation of bilirubin interaction with HSA's lysines: First electrostatic binding site in IIA subdomain. *Biophys.*

- Chem.* **2007**, *125*, 375-387. DOI: 10.1016/j.bpc.2006.09.013.
- [7] Sudlow, G.; Birkett, D. J.; Wade, D. N., The characterization of two specific drug binding sites on human serum albumin. *Mol. Pharmacol.* **1975**, *11*, 824-832.
- [8] Fehske, K. J.; Müller, W. E.; Wollert, U., The location of drug binding sites in human serum albumin. *Biochem. Pharmacol.* **1981**, *30*, 687-692. DOI: 10.1016/0006-2952(81)90151-9.
- [9] Honoré, B., Conformational changes in human serum albumin induced by ligand binding. *Pharmacol. Toxicol.* **1990**, *66*, 1-26. DOI: 10.1111/j.1600-0773.1990.tb01608.x.
- [10] Sollene, N. P.; Means, G. E., Characterization of a specific drug binding site of human serum albumin. *Mol. Pharmacol.* **1979**, *15*, 754-757.
- [11] He, X. M.; Carter, D. C., Atomic structure and chemistry of human serum albumin. *Nature*, **1992**, *358*, 209-215. DOI: 10.1038/358209a0.
- [12] Carter, D. C.; Ho, J. X., Structure of serum albumin. *Adv. Protein. Chem.* **1994**, *45*, 153-203. DOI: 10.1016/S0065-3233(08)60640-3.
- [13] Sugio, S.; Kashima, A.; Mochizuki, S.; Noda, M.; Kobayashi, K., Crystal structure of human serum albumin at 2.5 angstrom resolution. *Protein. Eng.* **1999**, *12*, 439-446. DOI: 10.1093/protein/12.6.439.
- [14] Sudlow, G.; Birkett, D. J.; Wade, D. N., Further characterization of specific drug binding sites on human serum albumin. *Mol. Pharmacol.* **1976**, *12*, 1052-1061.
- [15] Sjöholm, I.; Ekman, B.; Kober, A.; Ljungstedt-Pahlman, I.; Seiving, B.; Sjödin, T., Binding of drugs to human serum albumin: XI. The specificity of three binding sites as studied with albumin immobilized in microparticles. *Mol. Pharmacol.* **1979**, *16*, 767-777.
- [16] Sollene, N. P.; Means, G. E., Characterization of a specific drug binding site of human serum albumin. *Mol. Pharmacol.* **1979**, *14*, 754-757.
- [17] Ràfols, C.; Zarza, S., Molecular interactions between some non-steroidal anti-inflammatory drugs (NSAID's) and bovine (BSA) or human (HSA) serum albumin estimated by means of isothermal titration calorimetry (ITC) and frontal analysis capillary electrophoresis (FA/CE). *Talanta.* **2014**, *130*, 241-250, DOI: 10.1016/j.talanta.2014.06.060.
- [18] Moore, R. A.; Tramer, M. R.; Carroll, D.; Wiffen, P. J.; McQuay, H. J., Quantitative systematic review of topically applied non-steroidal anti-inflammatory drugs. *Brit. Med. J.* **1998**, *316*, 333-338. DOI: 10.1136/bmj.316.7128.333.
- [19] Bennett, J. S.; Daugherty, A.; Herrington, D.; Greenland, P.; Roberts, H.; Taubert, K. A., The use of Nonsteroidal Anti-Inflammatory Drugs (NSAIDs): a science advisory from the American Heart Association. *Circulation* **2005**, *111*, 1713-1716, DOI: 10.1161/01.CIR.0000160005.90598.41.
- [20] Baigent, C.; Patrono, C., Selective Cyclooxygenase 2 Inhibitors: Aspirin, and Cardiovascular Disease, *A Reappraisal. Arthritis & Rheumatism.* **2003**, *48*, 12-20, DOI: 10.1002/art.10738.
- [21] Tajmir-Riahi, H. A., An overview of drug binding to human serum albumin: Protein folding and unfolding. *Scientia Iranica*, **2007**, *14*, 87-95.
- [22] Kanakis, C. D.; Tarantilis, P.; Polissiou, M. G.; Diamantoglou, S.; Tajmir-Riahi, H. A., Antioxidant avonoids bind human serum albumin. *J. Mol. Struct.* **2006**, *98*, 69-74. DOI: 10.1016/j.molstruc.2006.03.051.
- [23] Gaudreau, S.; Neault, J. F.; Tajmir-Riahi, H. A., Interaction of AZT with human serum albumin studied by capillary electrophoresis, FTIR and CD spectroscopic methods. *J. Biomol. Struct. Dyn.* **2002**, *19*, 1007-1014. DOI: 10.1080/07391102.2002.10506804.
- [24] Neault, J. F.; Novetta-delen, A.; Arakawa, H.; Malonga, H.; Tajmir-Riahi, H. A., The effect of aspirin-HSA complexation on the protein secondary structure. *Can. J. Chem.* **2000**, *78*, 291-296. DOI: 10.1139/v00-003.
- [25] Purcell, M.; Neault, J. F.; Tajmir-Riahi, H. A., Interaction of taxol with human serum albumin. *Biochem. Biophys. Acta.* **2000**, *1478*, 61-68. DOI: 10.1016/S0167-4838(99)00251-4.
- [26] Ivanov, A. I.; Christodoulou, J.; Parkinson, A. J.; Barnham, K. J.; Tucker, A.; Woodrow, J.; Sadler, P. J., Cisplatin binding sites on human albumin. *J. Biol. Chem.* **1998**, *273*, 14721-14730. DOI: 10.1074/

- jbc.273.24.14721.  
 [27] Ahmed Ouameur, A.; Marty, R.; Tajmir-Riahi, H. A., Human serum albumin complexes with chloro-phyll and chlorophyllin. *Biopolymers* **2005**, *77*, 129-136. DOI: 10.1002/bip.20173.  
 [28] Hui, X.; Xiao-Dong, Y.; Xu-Dong, L.; Hong-Yuan, C., Determination of binding constants for basic drugs with serum albumin by affinity capillary electrophoresis with the partial filling technique. *Chromatographia*. **2005**, *61*, 419-422. DOI: 10.1365/s10337-005-0502-2.  
 [29] Artali, R.; Bombieri, G.; Calabi, L.; Del Pra, A., A molecular dynamics study of human serum albumin binding sites. *IL Farmaco*. **2005**, *60*, 485-495. DOI: 10.1016/j.farmac.2005.04.010.  
 [30] Li, J.; Zhu, X.; Yang, C.; Shi, R., Characterization of the binding of angiotensin II receptor blockers to human serum albumin using docking and molecular dynamics simulation. *J. Mol. Model.* **2010**, *16*, 789-798. DOI: 10.1007/s00894-009-0612-0.  
 [31] Sudhamalla, B.; Gokara, M.; Ahalawat, N.; Amooru, D. G.; Subramanyam, R., Molecular dynamics simulation and binding studies of  $\beta$ -sitosterol with human serum albumin and its biological relevance. *J. Phys. Chem. B*. **2010**, *114*, 9054-9062. DOI: 10.1021/jp102730p.  
 [32] Castellanos, M. M.; Colina, C. M., Molecular dynamics simulations of human serum albumin and role of disulfide bonds. *J. Phys. Chem. B*. **2013**, *117*, 11895-11905. DOI: 10.1021/jp402994r.  
 [33] Mozafari, E. S.; Tazikeh-Lemeski, E.; Saboury, A. A., Isothermal titration calorimetry and molecular dynamics simulation studies on the binding of indometacin with human serum Albumin. *Biomacromol. J*. **2016**, *2*, 21-30.  
 [34] Yang, F.; Bian, C.; Zhu, L.; Zhao, G.; Huang, Z.; Huang, M., Effect of human serum albumin on drug metabolism: Structural evidence of esterase activity of human serum albumin. *J. Struct. Biol.* **2007**, *157*, 348-355. DOI: 10.1016/j.jsb.2006.08.015.  
 [35] Pearlman, D. A.; Case, D. A.; Caldwell, J. W.; Ross, W. S.; Cheatham, T. E.; DeBolt, S.; Kollman, P. A., AMBER, a package of computer programs for applying molecular mechanics, normal mode analysis, molecular dynamics and free energy calculations to simulate the structural and energetic properties of molecules. *Comput. Phys. Commun.* **1995**, *91*, 1-41. DOI: 10.1016/0010-4655(95)00041-D.  
 [36] Duan, Y.; Wu, C.; Chowdhury, S.; Lee, M. C.; Xiong, G.; Zhang, W.; Lee, T. A., Point-charge force field for molecular mechanics simulations of proteins based on condensed-phase quantum mechanical calculations. *J. Comput. Chem.* **2003**, *24*, 1999-2012. DOI: 10.1002/jcc.10349.  
 [37] Wang, J.; Wolf, R. M.; Caldwell, J. W.; Kollman, P. A.; Case, D. A., Development and testing of a general Amber force field. *J. Comput. Chem.* **2004**, *25*, 1157-1174. DOI: 10.1002/jcc.20035.  
 [38] Jorgensen, W. L.; Chandrasekhar, J.; Madura, J.; Klein, M. L., Comparison of simple potential functions for simulating liquid water. *J. Chem. Phys.* **1983**, *79*, 926-935. DOI: 10.1063/1.445869.  
 [39] Jakalian, A.; Bush, B. L.; Jack, D. B.; Bayly, C. I., Fast, efficient generation of high-quality atomic charges. AM1-BCC model: I. Method. *J. Comput. Chem.* **2000**, *21*, 132-146. DOI: 10.1002/(SICI)1096-987X(20000130)21:2<132::AID-JCC5>3.0.CO;2-P.  
 [40] Essman, U.; Perela, L.; Berkowitz, M. L.; Darden, T.; Lee, H.; Pedersen, G., A smooth particle mesh Ewald method. *J. Chem. Phys.* **1995**, *103*, 8577-8593. DOI: 10.1063/1.470117.  
 [41] Ryckaert, J. P.; Ciccotti, G.; Berendsen, H. J. C., Numerical integration of the cartesian equations of motion of a system with constraints: Molecular dynamics of n-alkanes. *J. Comput. Chem.* **1977**, *23*, 327-341.  
 [42] Martyna, G. J.; Hughes, A.; Tuckerman, M. E., Molecular dynamics algorithms for path integrals at constant pressure. *J. Chem. Phys.* **1999**, *110*, 3275. DOI: 10.1063/1.478193.  
 [43] The PyMOL Molecular Graphics System, Version 0.99rc6, DeLano Scientific LLC.  
 [44] Kirkwood, J. G., Statistical mechanics of fluid mixtures. *J. Chem. Phys.* **1935**, *3*, 300-313. DOI: 10.1063/1.1749657.  
 [45] Zwanzig, R. W., High-temperature equation of state by a perturbation method. I. Nonpolar gases. *J. Chem. Phys.* **1954**, *22*, 1420-1426. DOI: 10.1063/1.1740409.

- [46] Åqvist, J.; Medina, C.; Samuelsson, J. E.; A new method for predicting binding affinity in computer-aided drug design. *Protein. Eng.* **1994**, *7*, 385-391. DOI: 10.1093/protein/7.3.385.
- [47] Massova, I.; Kollman, P. A., Combined molecular mechanical and continuum solvent approach (MM-PBSA/GBSA) to predict ligand binding. *Perspect. Drug. Discov. Design.* **2000**, *18*, 113-135. DOI: 10.1023/A:1008763014207.
- [48] Kollman, P. A.; Massova, I.; Reyes, C.; Kuhn, B.; Huo, S.; Chong, L.; Cheatham, T. E., Calculating structures and free energies of complex molecules: combining molecular mechanics and continuum models. *Accounts Chem. Res.* **2000**, *33*, 889-897. DOI: 10.1021/ar000033j.
- [49] Sitkoff, D.; Sharp, K. A.; Honig, B., Accurate calculation of hydration free energies using macroscopic solvent models. *J. Phys. Chem.* **1994**, *98*, 1978-1988. DOI: 10.1021/j100058a043.
- [50] Sadiq, S. K.; Wright, D. W.; Kenway, O. A.; Coveney, P. V., Accurate ensemble molecular dynamics binding free energy ranking of multidrug-resistant HIV-1 proteases. *J. Chem. Inf. Model.* **2010**, *50*, 890-905. DOI: 10.1021/ci100007w.
- [51] Singh, N.; Warshel, A., Absolute binding free energy calculations: On the accuracy of computational scoring of protein–ligand interactions. *Proteins.* **2010**, *78*, 1705-1723. DOI: 10.1002/prot.22687.
- [52] Brooks, B. R.; Janezic, D.; Karplus, M.; Harmonic analysis of large systems. I. Methodology. *J. Comput. Chem.* **1995**, *16*, 1522-1542. DOI: 10.1002/jcc.540161209.
- [53] Wang, J.; Morin, P.; Wang, W.; Kollman, P. A., Use of MM-PBSA in reproducing the binding free energies to HIV-1 RT of TIBO derivatives and predicting the binding mode to HIV-1 RT of efavirenz by docking and MM-PBSA. *J. Am. Chem. Soc.* **2001**, *123*, 5221-5230. DOI: 10.1021/ja003834q.
- [54] Srinivasan, J.; Miller, J.; Kollman, P. A.; Case, D. A., Continuum solvent studies of stability of RNA hairpin loops and helices. *J. Biomol. Struct. Dyn.* **1998**, *16*, 671-682. DOI: 10.1080/07391102.1998.10508279.
- [55] Tazikheh-Lemeski, E., Binding Free Energy and the structural changes determination in hGH protein with different concentrations of copper ions (A molecular dynamics simulation study). *J. Theor. Comput. Chem.* **2016**, *15*, 1-18. DOI: 10.1142/S0219633616500450.
- [56] Onufriev, A.; Bashford, D.; Case, D. A., Modification of the Generalized Born model suitable for macromolecules. *J. Phys. Chem. B.* **2000**, *104*, 3712-3720. DOI: 10.1021/jp994072s.
- [57] Connolly, M. L., Analytical molecular surface calculation. *J. Appl. Crystallogr.* **1983**, *16*, 548-558. DOI: 10.1107/S0021889883010985.
- [58] Metz, A.; Pflieger, C.; Kopitz, H.; Pfeiffer-Marek, S.; Baringhaus, K. H.; Gohlke, H., Hot Spots and transient pockets: Predicting the determinants of small-molecule binding to a protein-protein interface. *J. Chem. Inf. Model.* **2011**, *52*, 120–133. DOI: 10.1021/ci200322s.
- [59] Kabsch, W.; Sander, C., Dictionary of protein secondary structure: pattern-recognition of hydrogen-bonded and geometrical features. *Biopolymers.* **1983**, *22*, 2577-2637. DOI: 10.1002/bip.360221211.
- [60] Rezaei Behbehani, G.; Saboury, A. A.; Barzegar, L., A Thermodynamic investigation of aspirin interaction with human serum albumin at 298 and 310 K. *J. Thermodyn. Catal.* **2011**, *2*, 107. DOI: 10.4172/2157-7544.1000107.
- [61] Huo, S.; Massova, I.; Kollman, P. A., Computational alanine scanning of the 1:1 human growth hormone-receptor complex. *J. Comput. Chem.* **2002**, *23*, 15-27. DOI: 10.1002/jcc.1153.
- [62] Tsui, V.; Case, D. A., Calculations of the absolute free energies of binding between RNA and metal ions using molecular dynamics simulations and continuum electrostatics. *J. Phys. Chem. B.* **2001**, *105*, 11314-11325. DOI: 10.1021/jp011923z.